COMMUNICATION

End-Capping Effect of a Narrow Bandgap Conjugated Polymer on Bulk Heterojunction Solar Cells

Jin Kuen Park, Jang Jo, Jung Hwa Seo, Ji Sun Moon, Yeong Don Park, Kwanghee Lee, Alan J. Heeger,* and Guillermo C. Bazan*

Organic solar cells based on π-delocalized conjugated polymers have attracted considerable interest due to their potential to enable solution processable and economically viable renewable energy conversion devices.[1–4] Progress has been demonstrated by taking advantage of the bulk heterojunction (BHJ) strategy, where typically narrow bandgap conjugated polymers are blended with fullerene derivatives so that the correct nanoscale phase-separated morphology is obtained to manage charge carrier generation and transport.[5–8] Conjugated polymers with backbones comprising alternating donor-acceptor (D/A) structural units frequently display desirable absorption characteristics to harvest the solar spectrum, together with energy levels that enable photoinduced charge transfer to the fullerene, while keeping sufficiently high open circuit voltages for better power conversion efficiencies. As a result a wide range of D/A copolymer systems have been integrated into BHJ solar cells and these devices exhibit some of the best power conversion efficiencies.[9–16]

Controlling the optoelectronic characteristics of the conjugated polymer component is only part of the material design challenge.[4,17] Small concentrations of structural defects are anticipated to influence the overall device performance. Studies on the widely examined P3HT polymer exist in the literature that highlight how the chemical nature of the end groups influences charge trapping, device hysteresis, intermolecular packing, and film morphology.[18,19] Indeed, examination of the synthetic details for the synthesis of narrow bandgap D/A

polymers shows that precautionary efforts are often taken by capping the chain ends with various functionalities, typically a conjugated segment that is similar to the main chain components.[20–23] However, there is little information on the degree to which such end-group modifications benefit device performance.

In this contribution, we report on the characterization of BHJ solar cells fabricated with polymers with essentially identical physical characteristics, i.e. structural units, except for the end group functionalities with the goal of establishing which parameters and device architectures are more greatly affected. Our focus is on the polymer poly[(4,4-didodecyldithieno[3,2-*b*:2',3'-*d*]silole)-2,6-diyl-*alt*-(2,1,3-benzothiadiazole)-4,7-diyl]. Two versions were targeted for study. The first material, **P1** in **Scheme 1**, was prepared via microwave-assisted Stille cross coupling polymerization between **M1** and **M2**, as reported in the literature.[9] Once the polymerization was complete, the reaction was quenched using methanol and the product was purified via Soxhlet extraction. **P1** thus likely contains residual unreacted stannyl and bromide functionalites at the end groups. A second version of the polymer, **P2**, was obtained similarly with **M1** and **M2**, except for the subsequent additions of 2-bromothiophene and 2-(tributylstanny) thiophene prior to quenching with methanol (Scheme 1). Substantial efforts were dedicated to obtain **P1** and **P2** in sufficiently high and similar average molecular weights in order to make a fair comparison of their performance in devices. Several **M1**:**M2** stoichiometric ratios were examined (1:1, 1.035:1, 1.045:1 and 1.06:1) and the closest highest number average molecular weights (M_n) were obtained at 1.045:1. These conditions led to $M_n = 32$ kg/mol with a polydispersity index (PDI) of 2.3 for **P1**, and $M_n = 30$ kg/mol and PDI $= 2.1$ for **P2** (see Supporting Information, Figure S1).

X-ray photoelectron spectroscopy (XPS) was used to probe differences in the composition of **P1** and **P2**.[24] Specific emphasis was made on probing peaks due to Sn and Br, which would be anticipated to be more prominent for **P1** samples. To reduce signal to noise ratio, all XPS data were acquired over a period of several hours. **Figure 1** shows core level XPS spectra in the region of (a) Br 3d and (b) Sn $3d_{5/2}$ for **P1** and **P2**. The presence of Sn and Br in the **P1** sample is evident, whereas none can be detected in the case of **P2**. All other peaks are similar in both polymers. The data are consistent with **P1** containing residual bromide and tin species, most reasonably at the end groups of the chain, and with the successful end-capping of **P2** with thiophene units.

Figure 2a shows that the UV–vis absorption spectra of chlorobenzene solutions containing **P1** or **P2** are nearly identical. Similar observations can be made for thin films of the

J. K. Park,[†] Dr. J. H. Seo, Dr. Y. D. Park, Prof. G. C. Bazan
Department of Chemistry & Biochemistry
Department of Materials
Center for Polymers and Organic Solids
University of California
Santa Barbara, CA 93106, USA
E-mail: bazan@chem.ucsb.edu
Dr. J. Jo,[†] J. S. Moon, Prof. A. J. Heeger
Department of Physics
Department of Materials
Center for Polymers and Organic Solids
University of California
Santa Barbara, CA 93106–5090, USA
E-mail: ajhe@physics.ucsb.edu
Prof. K. Lee
Heeger Center for Advanced Materials
Materials Science and Engineering
Gwangju Institute of Science and Technology (GIST)
Gwangju 500–712, Korea
[†] J.K.P. and J.J. made equal contributions to this work (co-first author).

DOI: 10.1002/adma.201004629
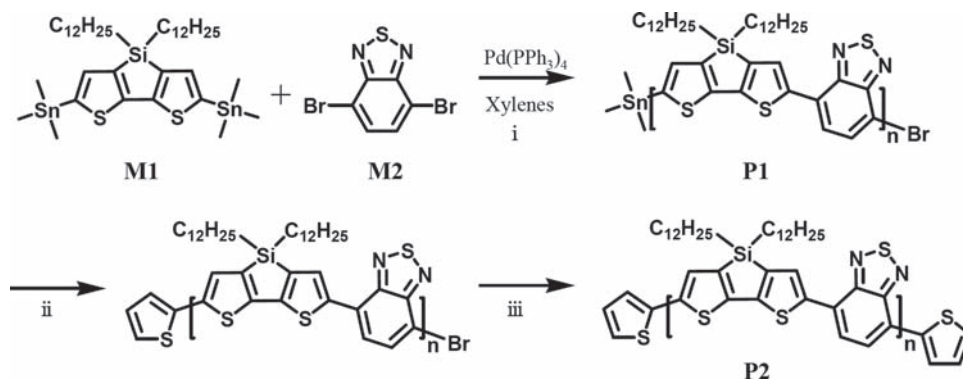
Scheme 1. The molecular structures and synthesis of **P1** and **P2**[a](i) 120 °C for 5 min, 140 °C for 5 min and 170 °C for 40 min throughout microwave reactor; (ii) degassed 4 equivalents of 2-bromothiophene; then microwave heating at same condition above; (iii) 8 equivalents of 2-(tributylstanny) thiophene under microwave heating.
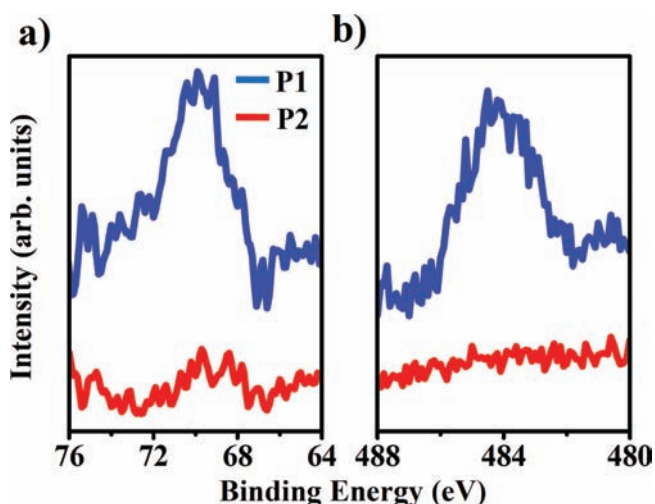

Figure 1. XPS spectra of (a) Br 3d and (b) Sn $3d_{5/2}$ for **P1** (blue) and **P2** (red)

polymers. However, the absorption onsets of the films are red-shifted by 15 nm relative to the solutions due to stronger interchain contacts and concomitant increase in electronic interaction between optical units. UV–vis spectra of blend films containing mixtures of **P1** or **P2**:[6,6]-phenyl C_{71} butyric acid methyl ester (PC$_{71}$BM) with a 1:1 weight ratio are also identical (see Supporting Information, Figure S2). This component ratio was chosen on the basis of previous optimization of blends used in solar cell devices.[9] The similarity of the emission spectra suggests that the end caps of polymer do not significantly alter intermolecular stacking and the electronic structure of the backbone.[9,18] Similar electronic structure similarities between **P1** and **P2** was further confirmed by ultra-violet photoemission spectroscopy (UPS) measurements, which exhibit no significant

change of the highest occupied molecular orbital energy (HOMO) levels (see Supporting Information, Figure S3). The **P1**:PC$_{71}$BM and **P2**:PC$_{71}$BM blends deposited under similar deposition conditions also show no obvious differences in morphology as determined by atomic force microscopy (AFM, Figure 2b, Figure 2c) and transmission electron microscopy (TEM, Figure 2d, Figure 2e).

The influence of end group modification in functioning devices was probed by fabricating a series of BHJ solar cells prepared by spin-coating **P1**:PC$_{71}$BM and **P2**:PC$_{71}$BM mixtures on substrates consisting of glass/ITO/poly(ethylenedioxythiophene):poly(styrene sulfonate) (PEDOT:PSS). A TiOx layer was then cast atop the BHJ layer. The rationale for this incorporation is the ability of the TiOx layer to improve the stability of solar cell devices.[25] Fabrication was completed by evaporation of an Al electrode. The BHJ layer thickness was controlled through changes in solution concentrations and spin-coating speeds. Further fabrication details can be found in the Experimental section.

It is worth pointing out that the sensitivity of power conversion efficiency to the active layer thickness is an important practical consideration for commercialization of the BHJ solar cells fabricated by large-area coating techniques.[26] Photoactive
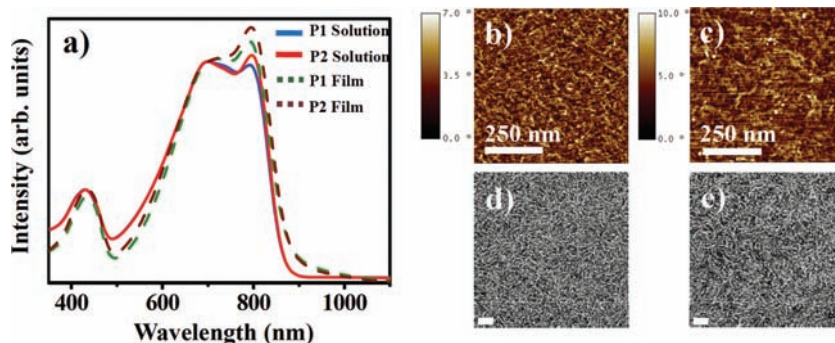

Figure 2. Absorption spectra(a) of dilute **P1** and **P2** in chlorobenzene (solid line) and absorption spectra of **P1** and **P2** films on glass substrate (dash line).Tapping mode AFM phase images of the blend films **P1**:PC$_{71}$BM(b) and **P2**:PC$_{71}$BM(c), and the TEM top-down images of blend films **P1**:PC$_{71}$BM (d), and **P2**:PC$_{71}$BM(e) previously deposited on ITO/PEDOT:PSS substrates at a 1:1 ratio. The scale bars for the TEM images are 100 nm.
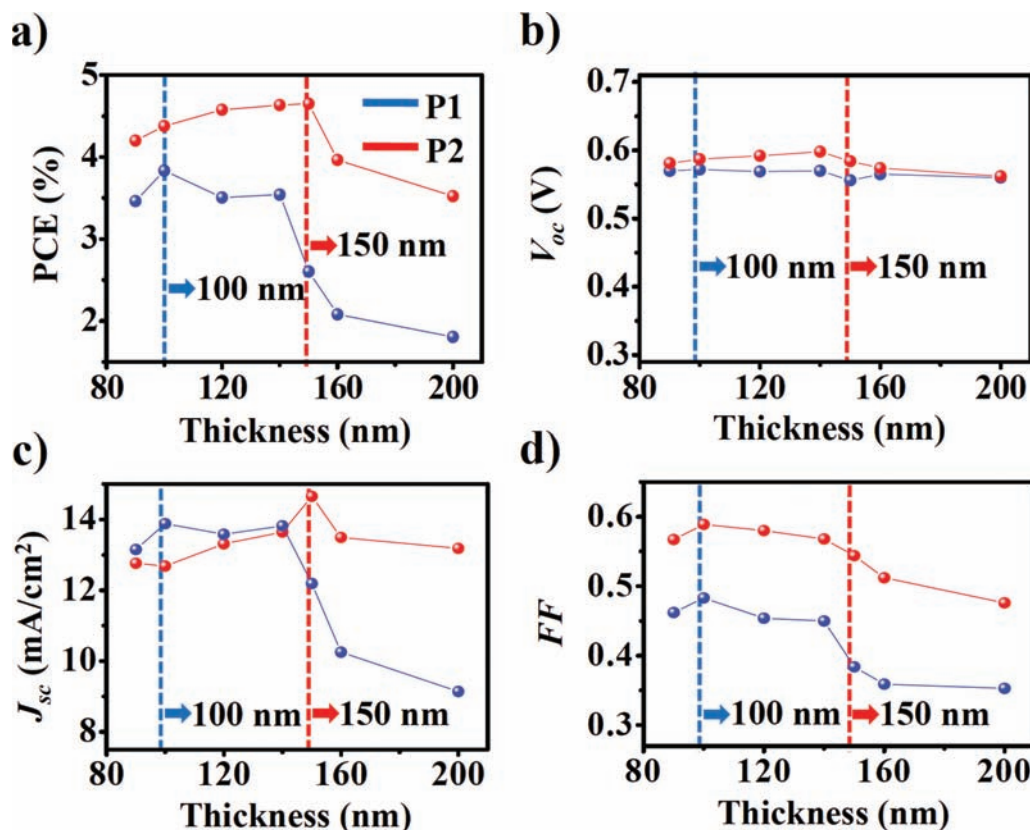
Figure 3. The BJH thickness dependency of photovoltaic performances such as (a) PCE, (b) V_{oc}, (c) FF and (d) J_{sc} of **P1**:PC$_{71}$BM and **P2**:PC$_{71}$BM devices. The optimal thickness is described by the dashed lines.

layers that can be increased in thickness while maintaining adequate fill factors (FF) are more desirable.[27] **Figure 3**a shows the power conversion efficiencies (PCEs) for **P1**:PC$_{71}$BM and **P2**:PC$_{71}$BM BJH devices as a function of active layer thickness. We first note that all devices with **P2** have better performances than those with **P1**. The open circuit voltage (V_{oc}) values of **P1** and **P2** devices are nearly invariant with varying thickness, as presented in Figure 3b. The **P2**:PC$_{71}$BM combination maintains relatively constant PCEs up to 150 nm thickness, at which point the highest current density (J_{sc}) was obtained (Figure 3c). For **P1**:PC$_{71}$BM, one observes a decrease in the PCE after 100 nm. We also note that similar improvements of **P2** relative to **P1** are found in devices where Al is deposited atop the BHJ layer, i.e. no TiOx layer (see Supporting Information, Figure S4). In view of the absence of differences in optical and morphological characteristics (Figure 2), we ascribe the more pronounced tendency for device performance deterioration to the greater accumulation of chain end defects in **P1**.

We further note that **P2**:PC$_{71}$BM layers also exhibit enhanced thermal stability. For these tests the BHJ layer was heated up to a specific temperature for 10 min prior to casting the TiOx layer. As shown in **Figure 4**a, the PCEs of the **P2**:PC$_{71}$BM devices gradually increase up to 150 °C (PCE = 4.7%) and collapse beyond 170 °C. Indeed, all the efficiency parameters obtained with **P2**:PC$_{71}$BM sustain constant values up to 150 °C (Figure 4a–d). In the case of **P1**:PC$_{71}$BM there is no beneficial effect by thermal

annealing; PCE decreases starting from 70 °C. Current density (J)–voltage (V) characteristics of the resulting optimized BHJ solar cells are shown in Figure 4e. **Table 1** provides a summary of the results. Values integrated from the external quantum efficiency (EQE) characteristics of the devices (Figure 4f) match the J_{sc} values with less than 4% error. As shown in Table 1, the **P2**:PC$_{71}$BM BHJ solar cell exhibits enhanced performance relative to the **P1**:PC$_{71}$BM device mainly due to an improved FF.

The series (R_s) and shunt resistance (R_{sh}) values obtained from J–V curves, measured in the dark condition can be found in Table 1. The **P2**:PC$_{71}$BM solar cells have lower R_s and higher R_{sh}, consistent with the higher FF of the **P2**:PC$_{71}$BM cells than **P1**:PC$_{71}$BM devices.[28,29] Therefore, end-capping (as in polymer **P2**) improves the device performance and thermal stability, most reasonably by decreasing the concentration of reactive chemical functionalities and structural defects.

In summary, we have used the narrow-bandgap conjugated copolymer, poly[(4,4-didodecyldithieno[3,2-*b*:2',3'-*d*]silole)-2,6-diyl-*alt*-(2,1,3-benzothiadiazole)-4,7-diyl], as obtained immediately after polymerization and after treatment with chain-end capping thiophene reagents, namely **P1** and **P2**, respectively, to gauge the impact of reactive end groups on the performances of BHJ solar cells. End-capping with thiophene improves performance by making the devices less sensitive to active layer thickness and to thermal degradation. We find that there is
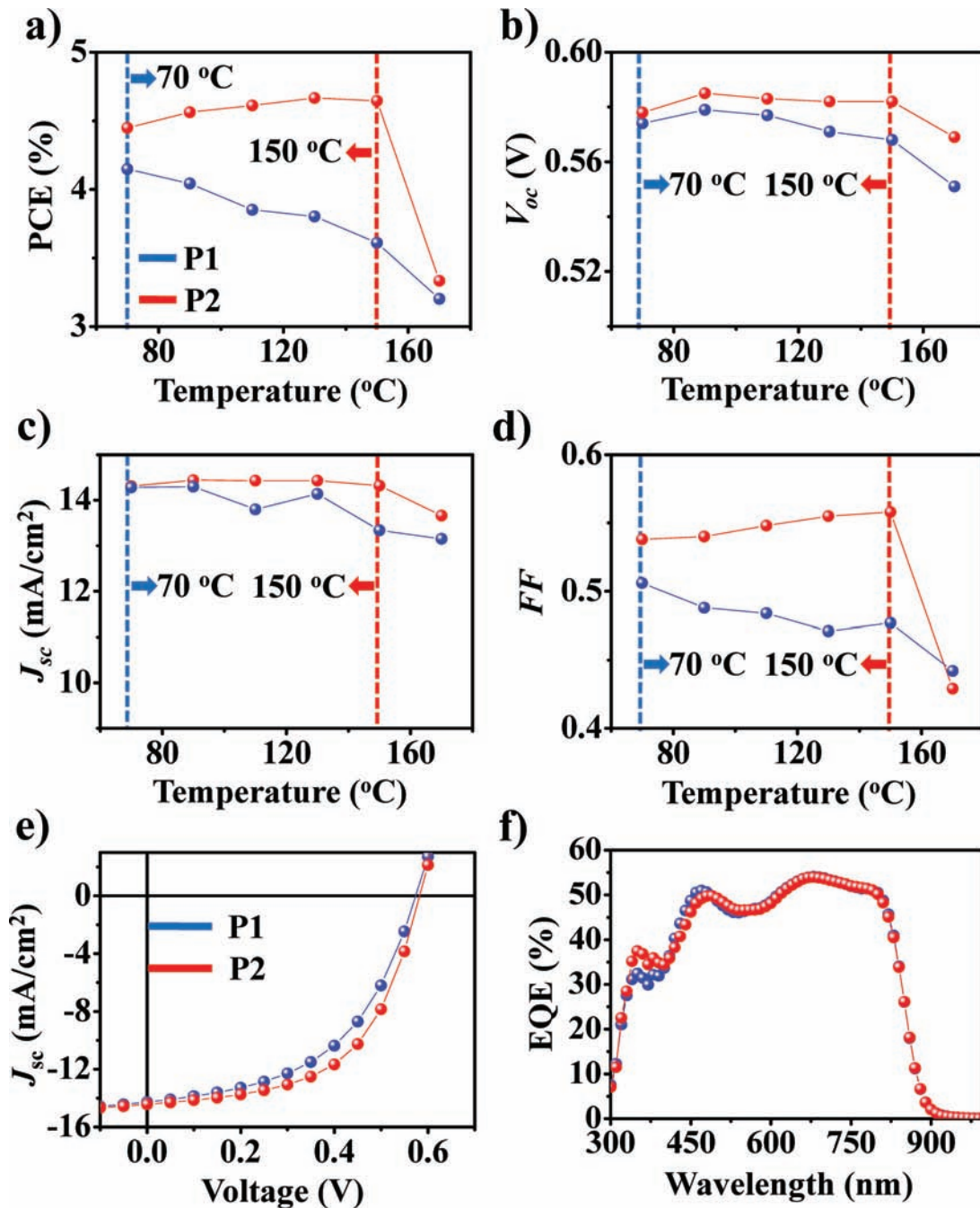
Materials
Views
www.MaterialsViews.com

ADVANCED
MATERIALS
www.advmat.de

COMMUNICATION

Figure 4. Effect of heating on (a) PCE, (b) V_{oc}, (c) J_{sc} and (d) FF of **P1**:PC$_{71}$BM and **P2**:PC$_{71}$BM devices at each optimal thickness (100 nm for **P1** devices and 150 nm for **P2** devices) and the summary of optimized photovoltaic characteristics of **P1**:PC$_{71}$BM (100 nm thickness and annealed at 70 °C) and **P2**:PC$_{71}$BM devices (150 nm thickness and annealed at 150 °C) described in (e) *J–V* characteristics obtained under AM 1.5G irradiation at 100 mWcm^{-2} and (f) the EQE spectra of same devices used in (e).

Table 1. Summary of device characterization.

	V_{oc} (V)	J_{sc} (mA/cm^2)	FF	PCE (%)	R_S (Ωcm^2)	R_{SH} (MΩ)	BHJ layer thickness	Annealing temperature
P1:PC$_{70}$BM	0.57	14.3 (14.9[a])	0.51	4.2	7.01	0.91	ca. 100 nm	70 °C
P2:PC$_{70}$BM	0.58	14.4 (14.9[a])	0.56	4.7	5.06	2.07	ca. 150 nm	150 °C

[a]J_{sc} values obtained from integration of EQE spectrum.

negligible difference in optical and morphological characteristics of the BHJ blends, which suggests that the chemical functionality affect adversely the electronic properties, most reasonably by behaving as charge carrier traps or by inducing undesirable chemical transformations under device operation. Such studies to understand the physical attributes of the BHJ components are important for transitioning fundamental research efforts into commercially viable technologies.

Experimental Section

Monomer synthesis: 5,5'*Bis*(trimethylstannyl)-3,3'-di-n-dodecylsilylene-2,2'-bithiophene (**M1**) and 4,7-dibromo-2,1,3-benzothiadiazole (**M2**) were prepared via literature procedures.[9]

Polymerization and end capping: To get the specific M_n, the stoichiometric ratio of distannyated **M1** and **M2** was adjusted. The ratios of **M1** and **M2** were 1:1, 1.035:1, 1.045:1, and 1.06:1. The exact weights of all chemicals were measured in a glovebox. To each microwave tube was added **M1** (300mg) and the corresponding amount of **M2** as determined by the stoichiometric ratio. Subsequently, Pd(PPh$_3$)$_4$ (13 mg) and xylenes (2 mL) were added. The tubes were then sealed inside of the glovebox and subjected to the following reaction conditions in a microwave reactor: 120 °C for 5 min, 140 °C for 5 min and 170 °C for 40 min. The resulting products were precipitated in methanol and filtrated. The residual solid was loaded into an extraction thimble and washed successively with hexane (4 h), THF (12 h), and acetone (30 min) and the insoluble portion of THF was collected. **P1** with M_n values of 20 kg/mol, 28 kg/mol, 32 kg/mol and 26 kg/mol as the equivalents of **M1** increased from 1.00 to 1.06 equivalents and each PDI was 1.9, 2.2, 2.4, and 2.3, respectively.

For end group modification, the specific stoichiometric ratios of **M1** and **M2** were determined as for **P1**. After polymerization, 4 equivalents of 2-bromothiophene relative to **M1** was added in the tube and was then subjected to the same polymerization conditions. Subsequently, 8 equivalents of 2-(tributylstanny)thiophene were added in the same tube and subjected to the same conditions as for the polymerization reaction. **P2** with M_n values of 20 kg/mol, 26 kg/mol, 30 kg/mol and 25 kg/mol as the equivalents of **M1** increased from 1.00 to 1.06 equivalents and each PDI was 1.9, 2.2, 2.1, and 2.2, respectively.

Device fabrication and characterization: Solar cell devices were fabricated on indium tin oxide (ITO)-coated glass substrates, which were previously cleaned by ultrasonication with detergent, deionized water, acetone, and isopropyl alcohol, sequentially. PEDOT:PSS (Baytron PH) was spin-cast onto the ITO-coated glass and then baked at 140 °C for 10 min in air. After transferring to a N$_2$-filled glovebox, the blend solution of polymer (**P1** or **P2**):PC$_{71}$BM (1:1 ratio by weight), which was dissolved in chlorobenzene (CB) with 4% chloronaphthalene by volume, was spin-castes onto the PEDOT:PSS layer. The BHJ layer thickness was controlled through changes in solution concentrations (1 to 2 wt%) and spin-coating speeds (1200 to 5000 rpm). All the thicknesses of BHJ films were determined by profilometry (AMBIOS, XP-100). The film was annealed for 10 min at various temperatures (70 to 170 °C) inside aN$_2$-filled glove box before depositing top electrodes. A TiOx precursor solution diluted (1:200 by volume) in methanol was spin-cast in air on top of the polymer:PC$_{71}$BM layer (5000 rpm, 40 s). The sample was heated at 80 °C for 10 min in air for hydrolysis. To complete the device fabrication, an Al electrode (100 nm) was deposited by thermal evaporation under high vacuum (<3 × 10^{-6} Torr). *J–V* curves were measured with a Keithley 2400 SMU while illuminated through an aperture (11.8 mm^2) with a simulated 100 mWcm^{-2} sunlight using a 300W Xe lamp with an AM1.5G filter. The EQE spectra were obtained by using a QE measurement system (PV measurements, Inc.).

TEM sample preparation: BHJ films were deposited by using spin-coating on glass/ITO/PEDOT:PSS substrates. To improve clarity of the images and to provide a fair comparison of the nanomorphology of **P1**:PC$_{71}$BM and **P2**:PC$_{71}$BM films, the active layer thickness was kept as close to ~100 nm as possible. To prepare the TEM specimens, the freestanding BHJ layers were floated on water and transferred to a Cu grid. Images were obtained from FEI Titan FEG High Resolution TEM operated at 300 kV. Both were defocused at about −30 μm.

Supporting Information

Supporting Information is available from the Wiley Online Library or from the author.

Acknowledgements

[1] C. J. Brabec, N. S. Sariciftci, J. C. Hummelen, *Adv. Funct. Mater.* **2001**, *11*, 15.

[2] G. Li, V. Shrotriya, Y. Yao, J. Huang, Y. Yang, *J. Mater. Chem.* **2007**, *17*, 3126.

[3] K. M. Coakley, M. D. McGehee, *Chem. Mater.* **2004**, *16*, 4533.

[4] M. C. Scharber, D. Wuhlbacher, M. Koppe, P. Denk, C. Waldauf, A. J. Heeger, C. L. Brabec, *Adv. Mater.* **2006**, *18*, 789.

[5] J. Peet, J. Y. Kim, N. E. Coates, W. L. Ma, D. Moses, A. J. Heeger, G. C. Bazan, *Nat. Mater.* **2007**, *6*, 497.

[6] J. K. Lee, W. L. Ma, C. J. Brabec, J. Yuen, J. S. Moon, J. Y. Kim, K. Lee, G. C. Bazan, A. J. Heeger, *J. Am. Chem. Soc.* **2008**, *130*, 3619.

[7] J. Peet, C. Soci, R. C. Coffin, T. Q. Nguyen, A. Mikhailovsky, D. Moses, G. C. Bazan, *Appl. Phys. Lett.* **2006**, *89*, 252105.

[8] Y. Liang, D. Feng, Y. Wu, S. T. Tsai, G. Li, C. Ray, L. Yu, *J. Am. Chem. Soc.* **2009**, *131*, 7792

[9] R. C. Coffin, J. Peet, J. Rogers, G. C. Bazan, *Nat. Chem.* **2009**, *1*, 657

[10] C. Piliego, T. W. Holcombe, J. D. Douglas, C. H. Woo, P. M. Beaujuge, M. J. Frechet, *J. Am. Chem. Soc.* **2010**, *132*, 7595.

[11] Y. Zou, A. Najari, P. Berrouard, S. Beaupre, B. R. Aich, Y. Tao, M. Leclerc, *J. Am. Chem. Soc.* **2010**, *132*, 5330.

[12] J. Hou, H. Y. Chen, S. Zhang, G. Li, Y. Yang, *J. Am. Chem. Soc.* **2008**, 16144.

[13] H. Y. Chen, J. Hou, S. Zhang, Y. Liang, G. Yang, Y. Yang, L. Yu. Y. Wu, G. Li, *Nat. Photonics.* **2009**, *3*, 649.

[14] C. V. Hoven, X. D. Dang, R. C. Coffin, J. Peet, T. Q. Nguyen, G. C. Bazan, *Adv. Mater.* **2010**, *22*, E63.

[15] J. C. Bijleveld, M. Shahid, J. Gilot, M. M. Wienk, R. A. J. Janssen, *Adv. Funct. Mater.* **2009**, *19*, 3262.

[16] J. Jo, D. Gendron, A. Najari, J. S. Moon, S. Cho, M. Leclerc, A. J. Heeger, *Appl. Phys. Lett.* **2010**, *97*, 203303.

[17] K. Vandewal, K. Tvingstedt, A. Gadisa, O. Inganäs, J. V. Manca, *Nat. Mater.* **2009**, *8*, 904.

[18] Y. Kim, S. Cook, J. Kirkpatrick, J. Nelson, J. R. Durrant, D. D. C. Bradley, M. Giles, M. Heeney, R. Hamilton, I. McCulloch, *J. Phys. Chem. C* **2007**, *111*, 8137.

[19] J. S. Kim, Y. Lee, J. H. Lee, J. H. Park, J. K. Kim, K. Cho, *Adv. Mater.* **2010**, *22*, 1355.

[20] N. Blouin, A. Michaud, D. Gendron, S. Wakim, E. Blair, R. N. Plesu, M. Belletete, G. Durocher, Y. Tao, M. Leclerc, *J. Am. Chem. Soc.* **2008**, *130*, 732.

[21] Y. Zou, D. Gendron, R. N. Plesu, M. Leclerc, *Macromolecules.* **2009**, *42*, 6361.

[22] F. Liang, J. Lu, J. Ding, R. Movileanu, Y. Tao, *Macromolecules* **2009**, *42*, 6107.

[23] P. T. Wu, H. Xin, F. S. Kim, G. Ren, S. A. Jenekhe, *Macromolecules.* **2009**, *42*, 8817.

[24] J. H. Seo, R. Yang, J. Z. Brzezinski, B. Walker, G. C. Bazan, T.Q. Nguyen, *Mater.* **2009**, *21*, 1006.

[25] K. Lee, J. Y. Kim, S. H. Park, S. H. Kim, S. Cho, A. J. Heeger, *Adv. Mater.* **2007**, *19*, 2445.

[26] P. Schilinsky, C. Waldauf, C. J. Brabec, *Adv. Funct. Mater.* **2006**, *16*, 1669.

[27] K. M. Coakley, M. D. McGehee, *Chem. Mater.* **2004**, *16*, 4533.

[28] J. Jo, S. I. Na, S. Kim, T. W. Lee, Y. Chung, S. J. Kang, D. Vak, D. Y. Kim, *Adv. Funct. Mater.* **2009**, *19*, 2398.

[29] J. H. Lee, S. Cho, A. Roy, H. T. Jung, A. J. Heeger, *Appl. Phys. Lett.* **2010**, *96*, 163303.

COMMUNICATION